International Journal of Heat and Fluid Flow 30 (2009) 751–760

Contents lists available at ScienceDirect

International Journal of Heat and Fluid Flow

journal homepage: www.elsevier.com/locate/ijhff

Enhanced heat transfer in confined pool boiling

C.M. Rops [a,*], R. Lindken [b], J.F.M. Velthuis [a], J. Westerweel [b]

[a] TNO Science & Industry, P.O. Box 155, 2600 AD Delft, The Netherlands
[b] Laboratory for Aero and Hydrodynamics, Delft University of Technology, The Netherlands

ARTICLE INFO

Article history:
Received 17 October 2008
Received in revised form 29 January 2009
Accepted 16 March 2009
Available online 23 April 2009

Keywords:
Pool boiling
Confinement
Heat transfer

ABSTRACT

We report the results of an experimental investigation of the heat transfer during nucleate boiling on a spatially confined boiling surface. The heat flux as a function of the boiling surface temperature was measured in pool boiling pots with diameters ranging from 15 mm down to 4.5 mm. It was found that a reduction of the pool diameter leads to an enhancement of the nucleate boiling heat flux for most of the boiling curve. Our experimental results indicate that this enhancement is not affected by the depth of the boiling pot, the material of the bounding wall, or the diameter of the inlet water supply. High-speed camera imaging shows that the heat transfer enhancement for the spatially confined pool boiling occurs in conjunction with a stable circulating flow, which is in contrast to the chaotic and mainly upward motion for boiling in larger pool diameters. An explanation for the enhancement of the heat transfer and the associated change in flow pattern is found in the singularisation of the nucleate boiling process.

1. Introduction

One the most effective heat transfer mechanisms provided by nature is the phase change of a liquid into a vapour during boiling. The basic heat transfer principles of the processes that occur during boiling are described in engineering text books such as Bell and Mueller (1984) or Schlünder et al. (1994). Rohsenow (1971) provides an overview of boiling phenomena occurring for pool boiling and flow boiling. A typical pool boiling curve (see eg. Carey, 1992; Dhir, 1998; Incropera and DeWitt, 2002) for water at atmospheric conditions is shown in Fig. 1, where the heat flux, q'', is given as a function of the wall superheat temperature ΔT. For increasing ΔT the boiling heat flux passes from the natural convection regime (for $\Delta T < 5$ K), through the nucleate boiling regime (for $5\text{ K} < \Delta T < \Delta T_C$), where the heat flux shows a strong increase with ΔT and reaches a maximum value $q''_{\max}$ at a critical superheat temperature $\Delta T_C \sim 25$ K. Above ΔT_C an unstable boiling regime exists, and the heat flux decreases when ΔT further increases. The increase of the heat flux with increasing ΔT in the nucleate boiling regime can be attributed to an increasing number of boiling sites that become activated (Dhir, 1998). The maximum in the heat flux occurs due to the increase of active boiling sites, which makes it increasingly difficult for the liquid to reach the superheated wall. For non-subcooled water at atmospheric pressure the critical heat flux is about 10^6 W/m^2, which is one of the highest attainable values for the heat flux.

Liquid flow has a strong influence on bubble growth and bubble departure size. Davis and Anderson (1966) developed a theoretical description for the incipience of nucleate boiling. This theory is based on the radius of the bubble nucleus, a balance of forces acting on the bubble, and the assumption of a linear temperature profile in the laminar sublayer.

The bubble departure frequency influences the nucleate boiling heat transfer. The faster the bubbles depart from the boiling surface, the larger their liquid 'pumping' action, which increases the heat flux from the wall towards the fluid. Although various descriptions can be found in literature, Demiray and Kim (2004) reports that transient conduction and/or micro convection was measured to be the dominant heat transfer mechanism. Myers et al. (2005) quantifies that not more than 23% of the total heat transfer can be attributed to microlayer evaporation and contact line heat transfer; see also Kim et al. (2006, Fig. 6). Basu et al. (2005) applies in their model the fundamental idea that all energy from the wall is first transferred to the liquid layer. From this superheated liquid layer, the energy is then transported into the vapour bubbles and the remainder of the bulk liquid.

An estimation based on the energy balance shows that the main heat transfer is not due to energy transport by the primary vapour bubbles, and therefore must be transported by the liquid phase. Based on the model of Bowring (1962), we state that the heat transport by the vapour bubbles leaving the active nuclei sites, Q''_{bubble}, is given by the expression:

$$Q''_{bubble} = \rho_{vap} \cdot V_{bubble} \cdot h_{ev} \cdot f \cdot N_a \tag{1}$$

where ρ_{vap} is the vapour density, V_{bubble} the volume of the departing vapour bubble, and h_{ev} the latent heat of evaporation of the fluid (J/kg). To estimate the maximum heat flux transported by the vapour

* Corresponding author. Tel.: +31 15 2692103; fax: +31 15 2692111.
E-mail address: cor.rops@tno.nl (C.M. Rops).

0142-727X/$ - see front matter © 2009 Elsevier Inc. All rights reserved.
doi:10.1016/j.ijheatfluidflow.2009.03.007

Nomenclature

A	boiling pot area (m^2)
c_d	drag coefficient (bubble: >0.4) (–)
D	diameter (m)
E	energy content of a vapour bubble (J)
f	frequency (Hz)
g	gravitational acceleration (9.81) (m/s^2)
h	heat transfer coefficient (W/m^2 K)
h_{ev}	latent heat of evaporation of the fluid (J/kg)
N_a	nucleation site density (m^{-2})
P	power (W)
q''	heat flux from the wall towards the fluid (W/m^2)
R	electrical resistance (Ω)
Q''_{bubble}	heat flux transported by bubbles (W/m^2)
T	temperature (K)
ΔT	difference between the boiling surface temperature and the fluid saturation temperature (K)
v	velocity (m/s)

Greek symbols

φ_{m_supply}	mass flow water supply boiling pot (kg/s)
λ	thermal conductivity (W/mK)
λ_T	Taylor wave length (m)
ρ	density (kg/m^3)
σ	surface tension (N/m)

Subscripts

0.2_diam	supply needle diameter 0.2 mm
0.35_diam	supply needle diameter 0.35 mm
0.5_diam	supply needle diameter 0.5 mm
bubble	vapour bubble
in	electrical input
liq	liquid
loss	heat losses to environment
max	maximum
sat	saturation
sub	subcooling
vap	vapour
w	wall, boiling surface

bubbles we estimate the departure frequency and the nucleation site density. As a first estimate we assume no vertical or lateral bubble coalescence, although Zhang and Shoji (2003) indicate a frequency increase by a factor of about 3–4 in case of vertical and lateral coalescence interaction. The departure frequency, f, is taken equal to the terminal rise velocity (with most likely a multiplication factor) of the vapour bubble, v_{bubble}, divided by the (theoretically) smallest possible distance between the centres of two rising bubbles, i.e. half the diameter of the first bubble plus half the diameter of the following bubble, D_{bubble}. We set the theoretical maximum value for the active nucleation site density, N_a, to the reciprocal value of the projected area of a single bubble, see also Kolev (2005). This leads to the following relation:

$$Q''_{bubble,\max} = \rho_{vap} \cdot 1/6\pi D^3_{bubble} \cdot h_{ev} \cdot \frac{v_{bubble}}{D_{bubble}} \cdot \frac{1}{1/4\pi D^2_{bubble}} = \sqrt{\frac{16\rho^2_{vap} g D_{bubble} h^2_{ev}}{27 c_d}} \quad (2)$$

where g is the standard gravitational acceleration (m/s^2), and c_d the drag coefficient of a rising bubble in a liquid (–). Using typical values for vapour bubbles in water ($\rho_{vap} \sim 1$ kg/m^3, $h_{ev} \sim 2.26$ MJ/kg, $D_{bubble} \sim 0.1$–2 mm, $c_d \sim 0.4$) the maximum heat flux is estimated to be of the order of 10^5 W/m^2. Therefore the highest achievable heat flux transported by vapour bubbles is approximately one order of magnitude less than the measured critical heat flux for water. This indicates that the main heat transport cannot be through non-coalescing vapour bubbles alone, but primarily through the induced liquid flow. The influence of coalescence with respect to our confined pool boiling experiment will be addressed further the discussion.

One of the first investigations on vapour bubble behaviour in pool boiling and the influence of liquid flow is conducted by Forster and Zuber (1955). They derive analytical expressions for growth rates and radii of the vapour bubbles. Bergles and Rohsenow (1964) examine in detail the boiling curve for forced convection. They find that the heat transfer for increasing flow velocities in the nucleate boiling regime is largely increased. More recently, Steiner et al. (2005) developed a detailed model to predict the bubble detachment time incorporating all forces (i.e., buoyancy, shear-lift, drag, and bubble growth) acting locally on the vapour bubble.

Kim et al. (2006) found that an increased vapour bubble departure frequency leads to an enhancement in the heat transfer. Zhao et al. (2003) establishes an increase in bubble departure frequency by placing a mesh screen above the heater, which leads to a forced coalescence of vapour bubbles. Wu et al. (1998) realises a reduction in the period of the vapour bubble generation cycle by adding a surfactant to the liquid. In all cases the increase of the bubble departure frequency leads to an enhancement in the nucleate boiling heat transfer.

Although the increased surface-to-volume ratio for scaling down devices generally improves the heat transfer, physical processes put a limit to the maximum achievable heat transfer rates. Bergles et al. (2003) investigates thermal management strategies with respect to the miniaturisation of devices, and points out the advantages of miniaturisation, such as a higher heat transfer coefficient and an enhancement of flow boiling. Disadvantages of miniaturisation are also mentioned, such as an increased pressure drop, the occurrence of flow instabilities, and manufacturing issues. The advantages and limitations of miniaturisation are reviewed by Kandlikar (2002, 2004).

The effect of reducing the heater size on the boiling heat transfer is investigated by Henry and Kim (2004). They find no influence on the heat transfer as a function of the heater size as long as the heater is sufficiently large (i.e., with an area of more than 1 mm^2). Only for the smallest heater size (0.8×0.8 mm^2) they find a reduction in heat flux, regardless of subcooling or gravity. They explain this decrease by limitations imposed on the size of a growing bubble and heater dryout. Kim et al. (2006) study the effect of the diameter of a wire heater during pool boiling. They also find a relatively small influence for their two largest heaters; However, their smallest wire heater (with a diameter of 25 μm) shows an enhancement in heat transfer. From their consecutive photo visualisation they attribute this enhancement to the smaller departing bubbles at a higher frequency. According to Kim et al. (2006) this higher frequency leads to an increase in the contribution from micro-convection heat transfer and a decrease in the contribution from latent heat transfer.

In the present paper we report our findings on nucleate boiling where not only the size of the heater plate is varied, but also where the size of the boiling pool is limited to the area of the heater. Confining the boiling pool limits the possibilities of the liquid flow to

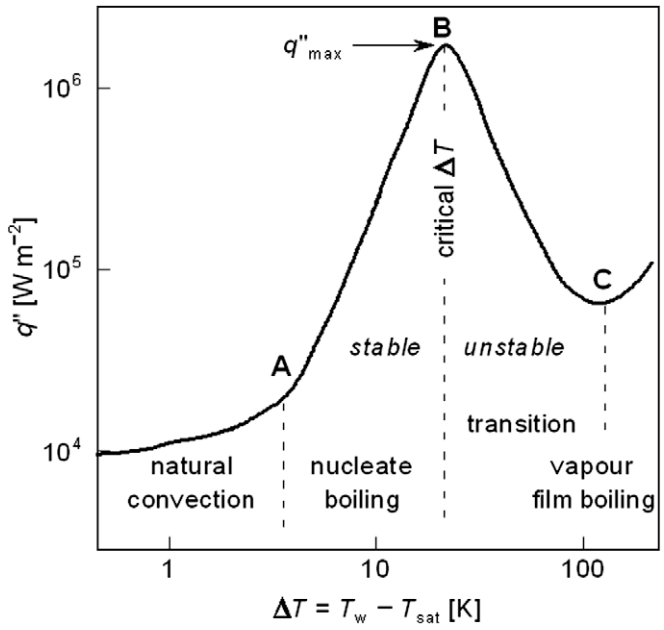

Fig. 1. Typical pool boiling curve at regular scale, which gives the surface heat flux q'' as a function of the difference ΔT between the wall temperature and the saturation temperature of the fluid, for water at atmospheric conditions.

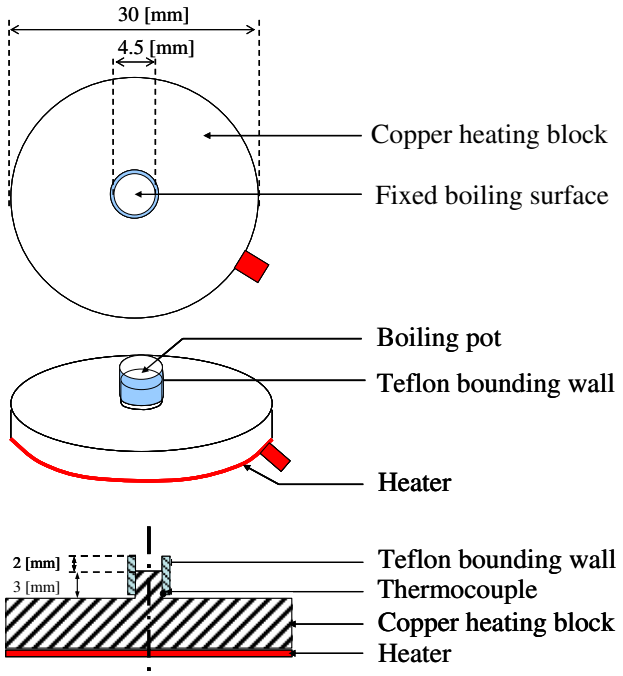

Fig. 2. Schematic overview of experimental setup for confined pool boiling; Top: top view; Middle: overhead view; Bottom: cross-section. A high boiling heat flux is ensured by the large size of the commercial heater placed at the bottom of a copper block. Similar experimental setups are made with a 5 mm, 6 mm, 8 mm, 10 mm and 15 mm boiling pot diameter.

reach the heated surface. If the width of the boiling pot is reduced, the number of active nucleation sites decreases as well. Therefore, as a first thought, one may expect that this leads to a decrease in heat transfer, as suggested by the observations by Henry and Kim (2004). Surprisingly, our observations indicate that a reduction of the boiling pot diameter results in a change in the fluid flow structure that induces an increase of the nucleate boiling heat transfer. By increasing the confinement effect of the boiling pot we achieved an increase of the measured heat transfer between 5 and 10 times in comparison with the heat transfer under non-confined boiling conditions.

In Section 2 we describe the measurement method, and in Section 3 the measurement results, as well as an error analysis of the experiments. A discussion of the results is given in Section 4, and a summary of the main results and conclusions is given in Section 5.

2. Measurement method

To investigate the nucleate boiling in a spatially confined geometry we performed measurements on the heat transfer in various confined boiling configurations. All measurement setups are constructed in a similar manner; therefore only the measurement set-up of the smallest pool boiling configuration is discussed here in detail.

2.1. Experimental setup and method

The heat transfer as a function of wall superheat for confined boiling is measured in a pool boiling configuration realised by a cylindrical Teflon bounding wall that is placed with a watertight seal around a small copper cylindrical shaped protrusion. A schematic of the experimental setup (for the smallest pool diameter of 4.5 mm) is shown in Fig. 2. Photographs of the setup are shown in Fig. 3.

The boiling surface has a diameter of 4.50 ± 0.05 mm with a heat conduction coefficient of $\lambda = 390$ W/mK (for copper). The cylindrical Teflon wall has a height of 2 mm and has a heat conduction coefficient of $\lambda \sim 0.3$ W/mK. This is much smaller than the heat conduction coefficient of the heating block, so that effectively the wall can be considered as non-conducting and all heat is dissipated at the bottom of the boiling pot.

The Teflon cylindrical wall is hydrophobic, and thus prevents the water from creeping out. A constant water supply ensures that the boiling pot remains completely filled during the measurements.

The boiling pot is positioned at the top of a larger copper heating block with an electrical heater on the bottom that can deliver a maximum heat flux of 45 kW/m^2. The copper heating block and the small copper cylindrical shaped protrusion are a single piece of pure copper. The boiling surface temperature is measured by a calibrated (temperature range: 80–125 °C) K-type thermocouple. A small horizontal carve is made in the small copper cylindrical shaped protrusion to accurately position the thermocouple. In order to avoid influence of the thermocouple on the boiling process it is located 2.5 ± 0.1 mm beneath the boiling surface. The thermocouple is in good thermal contact with the small copper cylindrical shaped protrusion and thermally insulated from the outside. The temperature of the boiling surface is deduced from the thermocouple reading and is corrected by taking into account the (one-dimensional) heat conduction in the bottom wall (see Section 2.2).

To keep the heat losses to a minimum, the set-up is properly insulated. Furthermore, the setup is covered in plastic to prevent the high temperature insulation material from wetting, and thereby reducing its insulating property (see Fig. 3B). The heat losses of the insulated set-up at steady state are determined in two separate experiments. In the first experiment the heat loss is determined as the amount of heat needed to maintain a stable temperature when no water is present in the boiling pot. The second experiment determines the heat loss from the difference of the electrical power input and the evaporation enthalpy of the inflowing water at steady state conditions. The heat loss through the insulation estimated by the two different methods was 1.50 ± 0.05 W. Although the dif-

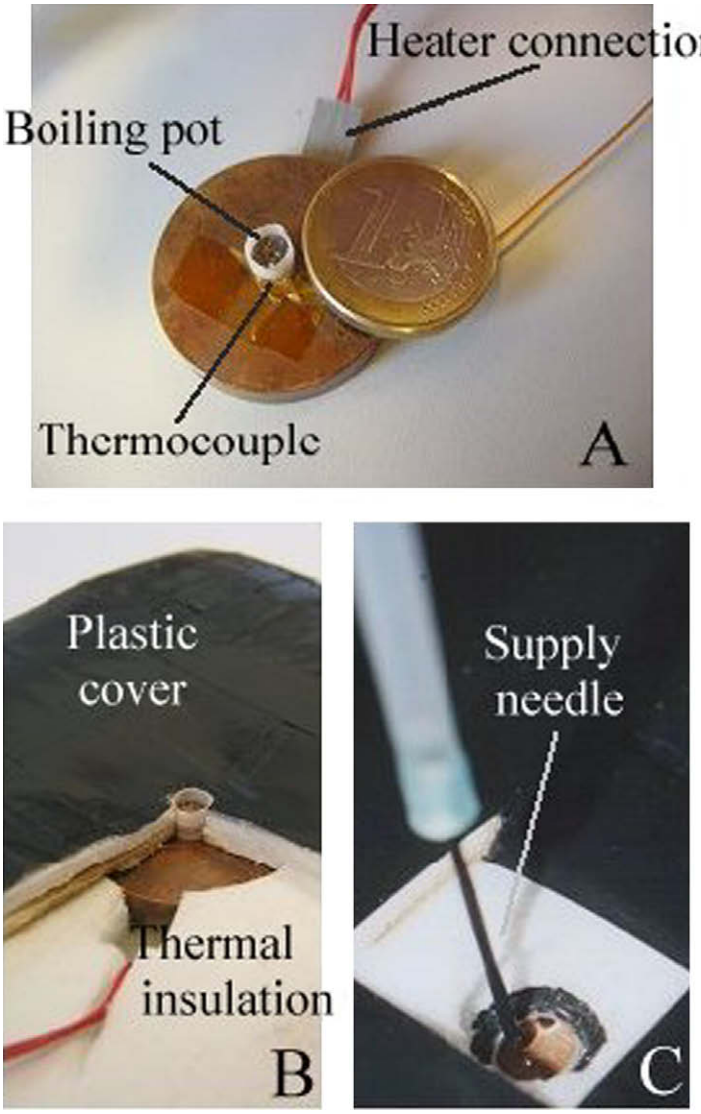

Fig. 3. The experimental set-up. A: copper heating block with 4.5 mm diameter cylindrical shaped protrusion and Teflon bounding ring; B: partly insulated boiling pot; C: insulated small-scale boiling pot and water supply.

ferent boundary condition in case of the "empty boiling pot method" leads to a more uniform temperature distribution in the copper heating block, the two measurements give the same result within a 0.05 W uncertainty. This indicates that the temperature distribution within the copper heating block is only a secondary effect which lies within the 0.05 W estimation precision. For higher wall superheats this heat loss increases in proportion to 1.78 ± 0.05 W. At higher wall superheats the heat loss could only be estimated by means of the "empty boiling pot method" (due to the splashing of the water the second method became unreliable). The precision of the heat loss estimation was constant for all measured wall superheats: 0.05 W, which corresponds to an apparent heat flux of 3×10^3 W/m^2. This amount is negligible with respect to the expected nucleate boiling heat fluxes of 10^5–10^6 W/m^2. The heat losses are estimated experimentally for each setup separately, for the complete range of researched wall superheats. The precision for all cases was within 0.05 W.

The heat flux, q'', from the wall to the fluid (W/m^2) is determined by the electrical input power to the heater at steady state conditions, i.e. when the exiting vapour flow is exactly balanced by the incoming water flow, and is given by:

$$Q'' = \frac{P_{in} - P_{loss}}{A} \tag{3}$$

where P_{in} is the measured heater power, P_{loss} the measured heat losses to the environment described previously (W), and A the surface area of the boiling pot (m^2). Using the above heat flux measurement method the electrical energy losses in the wires and the connections of the heater are included in the heat loss estimation and they do not influence the measurement. These heat losses are negligible, since the resistance of the heater ($R_{heater} = 28.8\Omega$) is much larger than the resistance of the wires plus connections ($R_{loss} \sim 0.1\Omega$).

The measurements are done by fixing the heat input. The temperature is measured with the thermocouple when the steady state lasts for at least 19 min. This time is equal to the time to fill or empty the smallest boiling pot at a mass flow rate of 0.1 g per hour (g/h). At equilibrium the temperature remains constant within 0.1 K. At the critical heat flux the incoming water mass flow rate is about 40 g per hour. To eliminate a possible hysteresis or aging effect or other influences introduced by the sequence of experiments, the heat transfer for a certain wall superheat is determined in a random order over a range of several days.

The constant water flow is provided by a flow controller (L1C2, Bronkhorst High-Tech) through a thin (0.35 mm diameter) Teflon-coated needle. The Teflon coating serves as insulation and minimises condensation of water on the needle. The needle is placed against the inner side of the cylindrical Teflon wall (see Fig. 3C) to prevent the formation of droplets at the tip of the needle. This ensures a constant flow of water with a temperature of 293 K.

All measurements of the various confined boiling configurations are conducted in the same manner with similar experimental set-ups, thus maintaining the 2 mm depth of the boiling pot for all diameters. The confined boiling surfaces are prepared identically, first by sanding the boiling surface and then by aging it with several hours of boiling.

2.2. Analysis of measurement assumptions

In this section we discuss the assumptions, approximations, and corrections that were applied in our experiments. These include: the difference between the measured temperature and actual surface temperature, subcooling due to the water supply, and errors due to splashing water droplets.

The surface temperature is determined from the temperature measured with a thermocouple located 2.5 mm below the surface. The surface temperature is determined by correcting the measured temperature for the heat conduction. Since the heat flux through the boiling surface is much higher than the heat losses along the small cylindrical shaped protrusion (see Fig. 2), the heat conduction is approximately one-dimensional. This one-dimensional approach is validated by means of a numerical solution of the temperature distribution in the copper block, taking into account the heat losses, that is shown in Fig. 4.

In the numerical solution the heat losses through the insulation are modelled by assuming a realistic value for the heat transfer coefficient of $h = 1\ \mathrm{W/m^2\,K}$. The temperature profile along the cylindrical pin is linear, which indicates that the heat transfer corresponds to a one-dimensional situation. The heat conductivity of the cylindrical pin estimated from the constant temperature slope along the pin varies within 3% of the actual value (390 W/m K), see Fig. 4. Even if the simulated heat transfer coefficient is raised to $h = 10\ \mathrm{W/m^2\,K}$, which corresponds to a non-isolated situation (Schlünder et al., 1994), the estimation error is within 5% at boiling heat fluxes above $1 \times 10^5\ \mathrm{W/m^2}$.

Special attention is given to locating the position of the thin thermocouple. The thermocouple is positioned parallel to the boiling surface, with an accuracy of 0.1 mm. The uncertainty in the distance between the thermocouple and the boiling surface results in an error in the estimation of the wall superheat. At a heat flux of $10^6\ \mathrm{W/m^2}$ the error in the wall superheat estimation is about 0.25 K. Therefore the total error margin of the wall superheat is within 0.5 K for all experiments.

The temperature of the liquid in the boiling pot is influenced by the temperature and the mass flow rate of the liquid water through the supply needle. The effect of subcooling is reduced by a proper mixing in the boiling pot. From high-speed camera visualisation we estimated that the mixing time less than 0.1 s. The water flow supply during a time interval equal to the estimated mixing time and the total mass of water present in the boiling pot determine the average liquid temperature. For example, in the case of the smallest boiling pot (with a liquid volume of $3.18 \times 10^{-8}\ \mathrm{m^3}$) and a liquid supply rate of 10 g/h (note that 40 g/h is the mass flow rate at CHF) the average liquid temperature is 99.3 °C. Zuber (Rohsenow, 1971) incorporated the effect of subcooling for the critical

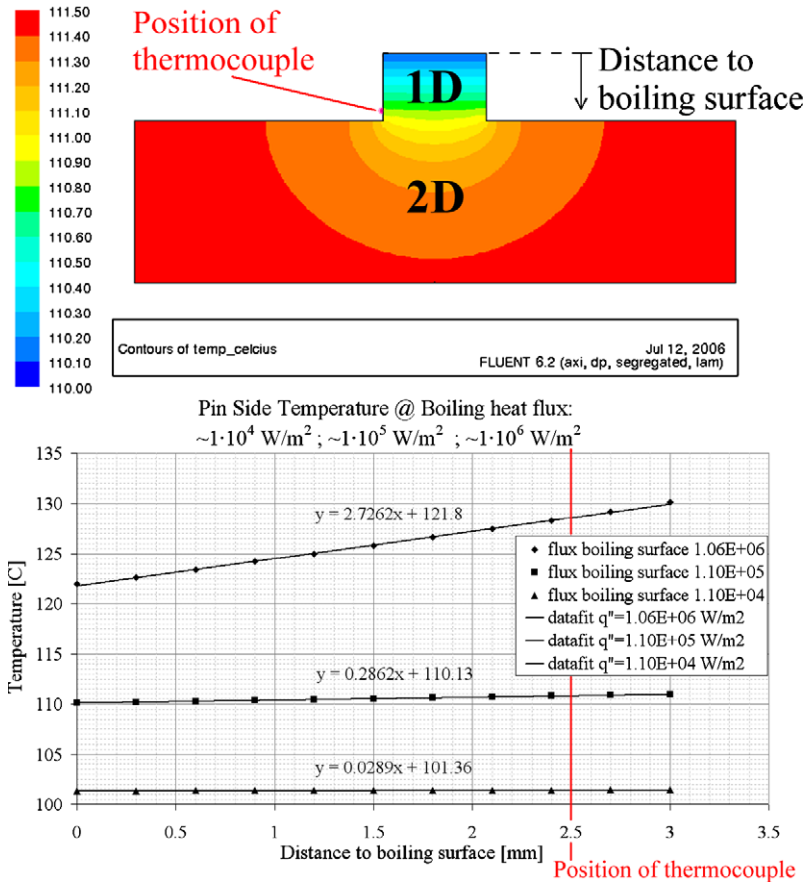

Fig. 4. The temperature distribution in the copper heater block (top) and temperature profiles for three heat loads of the copper block (bottom) from a numerical solution of the heat transfer (using the CFD code FLUENT). In all cases a linear temperature profile is found along the cylindrical shaped protrusion.

heat flux. For water at standard boiling conditions they give the following expression

$$\frac{q''_{sub}}{q''_{sat}} = 1 + 0.05 \cdot (T_{sat} - T_{liq}) \quad (4)$$

where q''_{sub} is the heat flux at subcooled conditions, and q''_{sat} the heat flux for saturated pool boiling. We assume that this relation, which holds at CHF, is also valid for the nucleate boiling regime. This means that for a liquid subcooling of two degrees or less, the heat flux will not be affected by more than 10%.

The splashing of liquid droplets has little or no effect on the measurement of the boiling curve, since the heat flux is determined from the electrical power input. In the superheat temperature range where we found the largest heat transfer enhancement (i.e., for $7 < \Delta T < 13$ K) the splashing is estimated to be less than 10% of the total water input. Only at higher wall superheat temperatures (i.e., $\Delta T > 13$ K) the splashing of droplets can lead to errors of about 30%.

Overviewing all error sources (such as uncertainties in the boiling surface area, in the surface temperature due to the actual position of the thermocouple, the electrical power input, the estimate of the heat loss, and the water subcooling) it is estimated that the combined error in the measured heat flux is about 15%. In the case that all errors simultaneously increase or decrease the measurement result, then the total measurement error is expected to be no greater than approximately 30%. This could lead to an uncertainty in the measured heat transfer enhancement factor of 1.3, which is well below the actually measured heat transfer enhancement of 5–10 times.

3. Results

3.1. Measurement results

The pool boiling curves measured for various pot diameters ranging from 4.5 to 15 mm are shown in Fig. 5.

The results shown in Fig. 5 indicate that a decrease of the diameter of the boiling area leads to an enhancement of the nucleate boiling heat flux. The boiling curve for the largest pool diameter (i.e., 15 mm) has a clear concave shape and is similar to the boiling curve for unconfined pool boiling (cf. Fig. 1). When the diameter of the boiling pool is reduced, the shape of the boiling curve becomes clearly convex, and we observe a significant increase in the measured heat transfer rate at intermediate values of the wall superheat temperature between 2 and 15 K (see Fig. 5). At small temperature differences between the boiling surface and the saturation temperature ($\Delta T \leqslant 2$ K), the heat fluxes for confined and unconfined pool boiling are equal and show the same trend. At $\Delta T \sim 3$ K the boiling curve for the small boiling pot starts to deviate from the unconfined pool boiling curve. The heat flux in the spatially confined geometry increases rapidly, and at wall superheats of 7–13 K the heat flux enhancement for the spatially confined nucleate boiling reaches a maximum value. Depending on the boiling pot diameter the confined heat flux is up to ten times higher than the heat flux in the case of unconfined pool boiling. At large wall superheats ($\Delta T > 20$ K) the confined pool boiling and unconfined pool boiling heat fluxes converge to the same value. The enhancement of the heat flux for confined pool boiling relative to the heat flux for unconfined pool boiling (i.e., the heat flux for the 15 mm diameter boiling pot) is displayed in Fig. 6.

In Fig. 7 we compare our results for the measured heat flux for the smallest (i.e., 4.5 mm diameter) and largest (i.e., 15 mm diameter) boiling pots against results published by others (Vinayak Rao and Balakrishnan, 2004; Raykoff and Kandlikar, 1997; Lee et al., 1994). The agreement between our results for the 15 mm diameter boiling pot (representing the unconfined boiling case) and those reported in the literature confirms the validity of our experimental approach for the measurement of the heat flux.

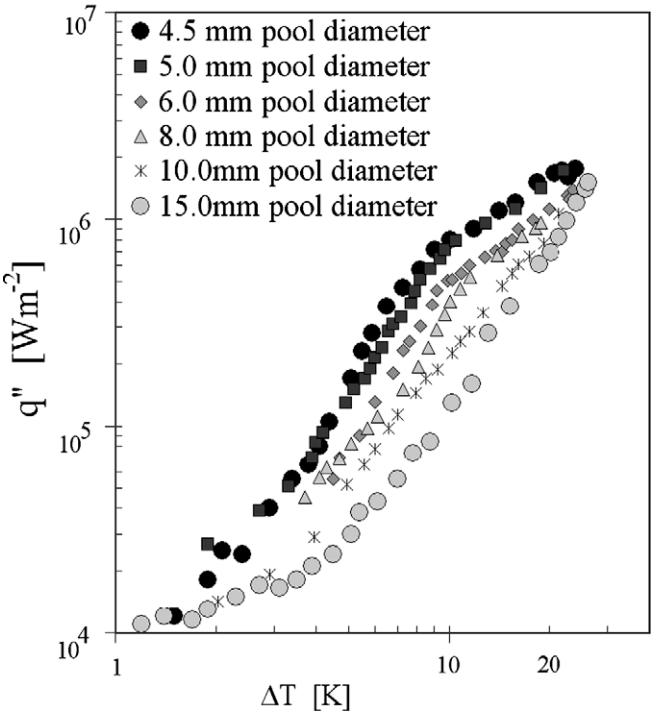

Fig. 5. Measured heat flux, q'', as a function of the difference ΔT between the wall temperature and the saturation temperature of the fluid for confined pool boiling. Experimental results are obtained for various boiling pot diameters between 4.5 mm and 15 mm. For the smallest boiling pool the heat transfer is increased by about ten times in comparison to the result for largest pool diameter Error margin horizontal axis: 0.5 K; Error margin vertical axis: 30%.

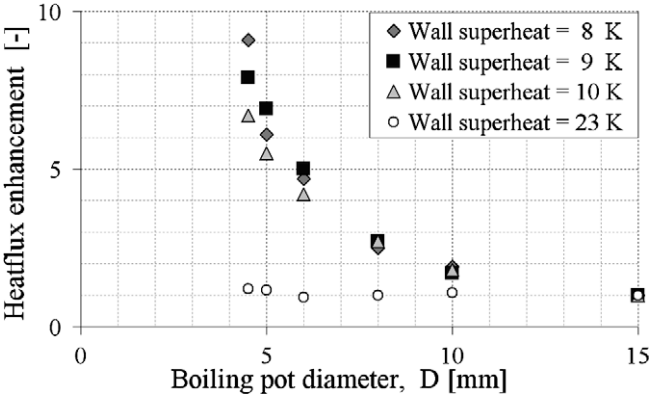

Fig. 6. The heat flux enhancement as function of the confinement by the boiling pot diameter at different wall superheat.

3.2. Variation of the measurement setup

To verify that our observation of the enhancement of the heat transfer for confined pool boiling is independent of geometry, the applied materials, and other conditions, several variations of the experimental configuration were carried out, namely:

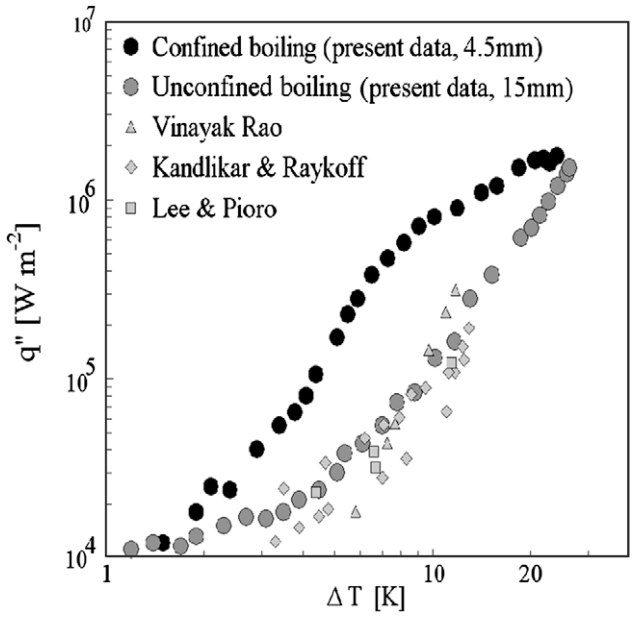

Fig. 7. Measured heat flux q' for confined and unconfined pool boiling as a function of the difference ΔT between the wall temperature and the saturation temperature of the fluid. Our experimental results for the 15 mm diameter boiling pot coincide with existing results, whereas our confined pool boiling result for the 4.5 mm boiling pot shows a significantly different behaviour. Error margin horizontal axis: 0.5 K; Error margin vertical axis: 30%.

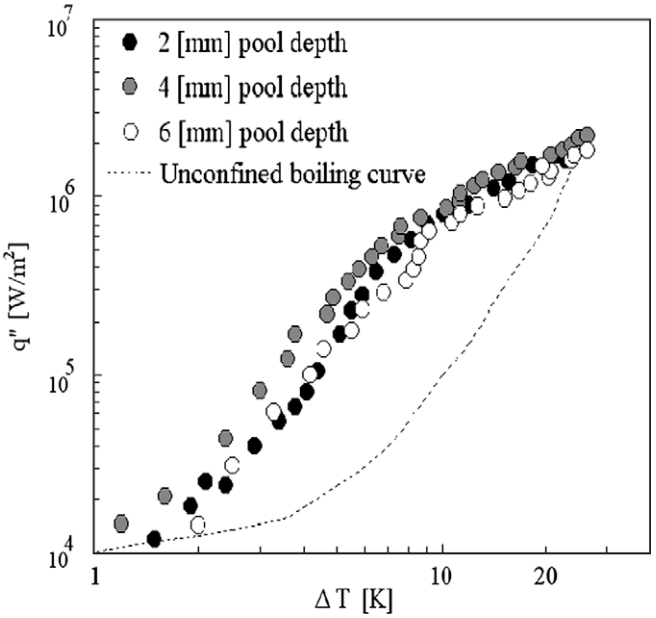

Fig. 8. Measured heat flux q'' for spatially confined boiling as a function of the difference ΔT between the wall temperature and the saturation temperature of the fluid. Experimental results for the three different pot depth. The dashed line represents the boiling curve for unconfined boiling. Error margin horizontal axis: 0.5 K; Error margin vertical axis: 30%.

1. variation in pot depth (or aspect ratio),
2. variation of the bounding wall material,
3. variation in the diameter of the inlet water supply.

To investigate the influence of the boiling pot depth two additional pool boiling pots were produced with pot depths of 4 mm and 6 mm, respectively. The results of this variation in the height of the bounding wall for 2 mm (indicated as "original"), 4 mm and 6 mm, are shown in Fig. 8.

Fig. 8 shows that the depth of the boiling pot has only a minor influence on the shape of the confined pool boiling curve. This indicates that there is no significant interaction between flow structures, heat transfer mechanism and boiling pot wall with respect to a variation in height.

The influence of the boiling pot wall material is investigated by changing the bounding wall material from hydrophobic (Teflon, nominal contact angle ~115°) to hydrophilic (PMMA, nominal contact angle ~70°). The boiling pot depth in this case is kept constant at 2 mm.

The boiling curve measured with a 2 mm high PMMA bounding wall in Fig. 9 shows a similar behaviour as the measurements using a 2 mm Teflon bounding wall. For low wall superheat temperatures no data points are shown since no stationary state could be identified within the 19-min time interval observed for all other data points.

The possible effect of the water in-flow velocity is investigated by altering the inner diameter of the supply needle (see Fig. 3C). We tested three needle diameters, i.e. 0.20 mm, 0.35 mm and 0.50 mm, which give mean flow velocities of 17 mm/s, 6 mm/s and 3 mm/s, respectively at a mass flow rate of 2 g/h. The results are shown in Fig. 10.

The results presented in Fig. 10 show that a variation of the needle diameter (i.e., inlet flow velocity) does not lead to significant differences in the result for the measured heat flux. This can be explained by the fact that the bubble velocities (with a typical value of $v_{bubble} \sim 0.1$ m/s) are approximately one order of magnitude larger than the liquid supply velocities. These bubble velocities are estimated by bubble tracking from digital high-speed recordings (see Section 3.3 below) of the bubbles that are visible from at the top of the boiling fluid and that correspond to values reported in the literature (Mingming and Morteza, 2002; Moghaddam and Kiger, 2004).

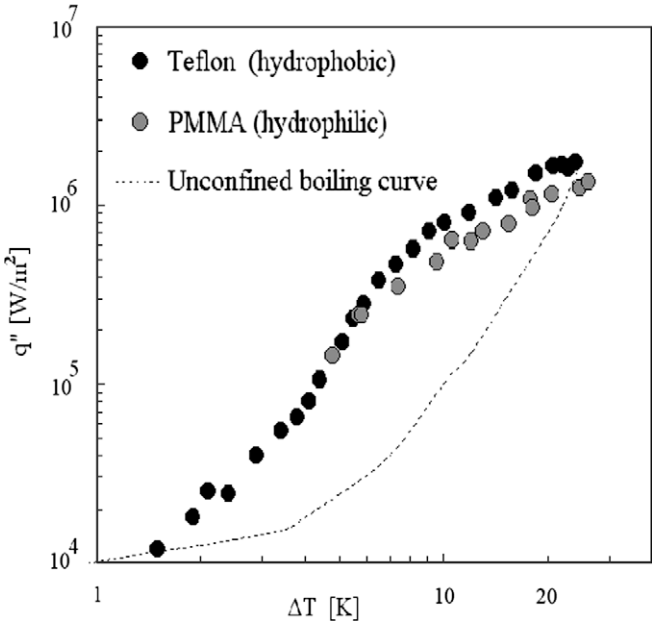

Fig. 9. Measured heat flux q'' for spatially confined boiling as a function of the difference ΔT between the wall temperature and the saturation temperature of the fluid. Experimental results for the two different bounding wall materials, i.e. hydrophobic (Teflon "original") and hydrophilic (PMMA). The dashed line represents the boiling curve for unconfined boiling. Error margin horizontal axis: 0.5 K; Error margin vertical axis: 30%.

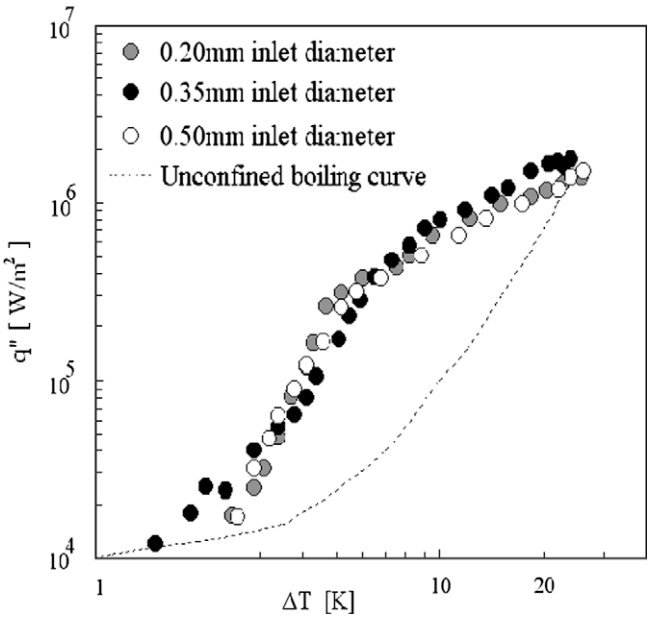

Fig. 10. Measured heat flux q'' for spatially confined boiling as a function of the difference ΔT between the wall temperature and the saturation temperature of the fluid. Experimental results for the various water supply diameters, i.e. 0.2 mm, 0.35 mm ("original") and 0.5 mm. The dashed line represents the boiling curve for unconfined boiling. Error margin horizontal axis: 0.5 K; Error margin vertical axis: 30%.

3.3. High-speed camera visualisation

From the analysis presented in the Introduction, it is conjectured that the confinement modifies the flow pattern in the boiling pot. We therefore investigated the spatially confined boiling by observing the flow patterns in the thin liquid layer for the unconfined (i.e. 15 mm diameter) and the smallest confined (i.e., 4.5 mm diameter) boiling pot with a high-speed video camera (Photron Ultima APX, with 1024 × 1024 pixels resolution at a framing rate of 1000 frames per second) that was equipped with a long-distance macro-lens (Rhodenstock). The camera was positioned at an angle of approximately 40°. This allowed us to view the flow at the top of the boiling fluid, while at the same time we could infer the vertical motion of the bubbles in the fluid. The large working distance of the camera lens of about 20 cm was applied to prevent vapour condensation on the lens. The motion of the bubble patterns was determined by tracking of the vapour bubbles.

Fig. 11 shows stills of the high-speed video that were observed at a wall superheat of 7 K (near the maximum enhancement in heat transfer; see Figs. 4 and 6). The high-speed video sequences show a structured and circulating flow for the spatially confined boiling set-up. In the unconfined boiling set-up (i.e., the 15 mm diameter boiling pot) we observed a more chaotic and mainly upward motion.

4. Discussion

As mentioned in the introduction, coalescence of vapour bubbles has a significant influence on the vapour bubble departure frequency and thus on the boiling heat flux. However the coalescence behaviour should not differ for a small boiling pot, and the suggested increase of by a factor 3–4 as given by Zhang and Shoji (2003) can not explain the observed enhancement of the heat flux for confined pool boiling.

The observed enhancement of the heat flux for confined pool boiling can be explained by a change in the flow pattern of the liquid for decreasing dimensions of the boiling pot. For unconfined pool boiling the chaotic and random motion of bubbles impedes the flow of cooler liquid towards the heated surface, whereas for confined pool boiling, the observations from the high-speed video indicates that the flow patterns changes to a structured and circulating motion of much smaller vapour bubbles. The circulating flow is driven by the rising vapour bubbles and directs the bulk liquid towards the superheated bottom. In the wake of the rising bubbles liquid is efficiently moved away from the heated surface, while in the gaps between the rising bubbles, due to conservation of mass, colder liquid flows towards the heated surface. The circulating flow sweeps the vapour bubbles more quickly, which leads to the creation of smaller vapour bubbles, yet at a higher departure fre-

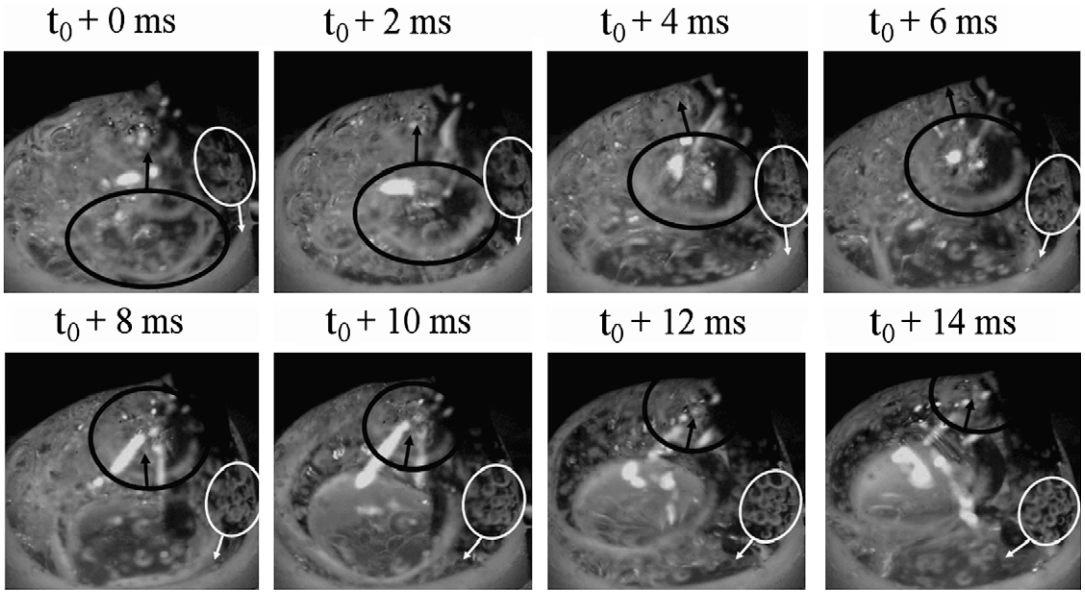

Fig. 11. Stills from the high-speed video visualisation (see supplementary electronic material) for the confined pool boiling (i.e., the 4.5 mm diameter boiling pot) at a wall superheat of 7 K. The black circles show the position of a bubble at the front side of the boiling pot, while the white circles mark the position of rear-side bubbles. The relative motion of the front and rear side bubbles indicate a circulating motion of the fluid.

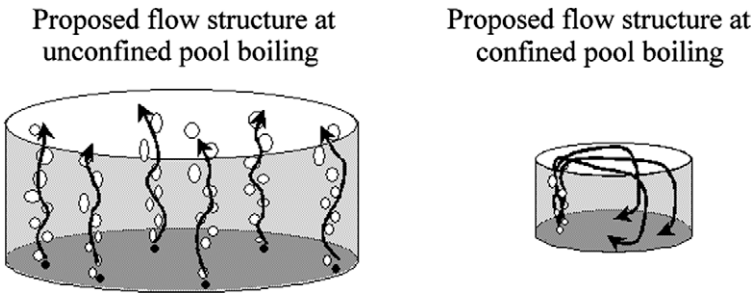

Fig. 12. Visualisation of hypothesis for explanation of existence of the circulating motion in confined pool boiling. Left: unconfined pool boiling situation, chaotic motion. Right: confined pool boiling situation, circulating flow.

quency. The wall-normal liquid entrainment at the boiling surface is enlarged and hence increases the heat transfer towards the fluid.

Based on the correlation of Chen (1963) an estimation is made of the increase in heat transfer seen due to forced convective boiling. The forced convective boiling heat transfer is estimated by the turbulent flow correlation given by Dittus and Boelter (1930) multiplied by a two-phase multiplier. For the observed bubble velocities at 7 K wall superheat and taking the diameter of the boiling pot as the characteristic length, the turbulent flow heat flux is about $3 \times 10^4\,\mathrm{W/m^2}$. Although it is not possible to calculate the two-phase multiplier for our case, in practice its value readily exceeds 10. Therefore the measured heat transfer enhancement in the confined pool boiling experiment is similar to the above estimated forced convective boiling heat flux.

Kandlikar (2002) investigated the influence of the liquid flow on the bubble growth and departure size, and he showed that an increased flow leads to smaller bubble departure sizes and a faster bubble growth. Kim et al. (2006) and others (Wu et al., 1998; Zhao et al., 2003) noted that an increased bubble departure frequency leads to an increase in heat transfer. These observations are in support of our explanation of the heat flux enhancement for confined pool boiling.

To explain the change in flow pattern, we consider the detailed nucleation process of the vapour bubbles. In the nucleate boiling regime the vapour bubbles grow and depart from specific locations, called nucleation sites. The origin of the stable circulating motion may be found in the nucleation site density, which is the number of active nucleation sites per unit area. Qi and Klausner (2006) report 13 active sites per square centimetre at the start of the nucleate pool boiling regime for water and copper. Basu et al. (2002) mention similar active nucleation site densities in case of flow boiling. At increasing wall temperature the nucleation number density grows about two orders of magnitude (Benjamin and Balakrishnan, 1997; Sakashita and Kumada, 2001; Basu et al., 2002). Consequently, only very few, and possibly just one, active sites are present in our experiments for the spatially confined boiling measurements, while for the unconfined boiling set-up a tenfold of active sites are present.

Fig. 12 (left) schematically shows the chaotic motion induced by the multiple nucleation sites at unconfined pool boiling. The image on the right visualises how the singularisation of the nucleation in confined pool boiling allows the formation of only a few or maybe even a single bubble column above the active nucleation site that acts as a stable driving mechanism for a steady circulating motion.

At larger wall superheats more nucleation sites become active in the confined pool boiling pot as well. As a result, the circulating flow pattern breaks down as multiple bubble columns counteract each other. Similar pattern formation can be observed in macroscopic bubble columns (Mudde, 2005). The pattern breakdown leads to a decrease of the enhancement effect and the confined boiling heat flux approaches the conventional critical heat flux for unconfined pool boiling.

5. Conclusions

Our results demonstrate an enhancement of the nucleate boiling heat flux when the boiling pot diameter is decreased. The decrease in the size of the pool boiling pot results in what we call 'confined pool boiling' (Fig. 5). With our analysis of possible errors and a variation of experimental parameters we could exclude that the observed enhancement is the result of a variation in boiling pot depth, the material of the bounding wall, or the variation in the diameter of the inlet water supply. In the nucleate boiling regime, at wall superheats of $\Delta T \sim 7\text{-}13$ K, the heat flux in confined boiling is almost ten times higher than the heat flux for unconfined pool boiling (Fig. 5). An explanation is found in the singularisation of the basic process for nucleate pool boiling, leading to different flow behaviour. The flow pattern is chaotic in the case of unconfined pool boiling, and it becomes directed and circulating as the dimensions of the confinement are reduced. The circulating fluid motion augments the entrainment of liquid by the vapour bubbles, and hence it significantly increases the heat transfer in the nucleate boiling regime. Therefore, for temperatures below the CHF, the heat flux does not show a rapid decrease. This allows an operation of the device at a comfortable temperature safety margin with respect to the critical superheat temperature (see Fig. 1) without compromising too much in heat transfer capacity. When confined boiling would be integrated on a large scale (by means of 'numbering up' or 'scaling out'), it has the potential of improving the heat transfer efficiency while remaining the same temperature safety margins in industrial facilities and home appliances.

Acknowledgements

The contributions of J.P. van der Dennen, M. Oitrou and M.M. Dauda to the heat transfer experiments is greatly appreciated.

Appendix A. Supplementary material

Supplementary material associated with this article can be found, in the online version, at doi:10.1016/j.ijheatfluidflow.2009.03.007.

References

Basu, N., Warrier, G.R., Dhir, V.K., 2002. Onset of nucleate boiling and active nucleation site density during subcooled flow boiling. J. Heat Transfer 124, 717–728.

Basu, N., Warrier, G.R., Dhir, V.K., 2005. Wall heat flux partitioning during subcooled flow boiling: part 1-Model development. J. Heat Transfer 127, 131–140.

Bell, K.J., Mueller, A.C., 1984. Wolverine Engineering Data Book II. Wolverine Division of UOP Inc..

Benjamin, R.J., Balakrishnan, A.R., 1997. Nucleation site density in pool boiling of saturated pure liquids: effect of surface microroughness and surface liquid physical properties. Exp. Therm. Fluid Sci. 15, 32–42.

Bergles, A.E., Rohsenow, W.M., 1964. The determination of forced-convection surface-boiling heat transfer. J. Heat Transfer 86, 365–372.

Bergles, A.E., Lienhard, J.H., Kendall, G.E., Griffith, P., 2003. Boiling and evaporation in small diameter channels. Heat Transfer Eng. 24 (1), 18–40.

Bowring, R.W., 1962. Physical Model based on Bubble Detachment and Calculation of Steam Voidage in the Subcooled Region of a Heated Channel. HPR-10, Institute for Atomenergi, Halden, Norway.

Carey, V.P., 1992. Liquid–Vapor Phase Change Phenomena. Taylor & Francis, London, UK.

Chen, J.C., 1963. A correlation for boiling heat transfer to saturated fluid in convective flow. ASME Paper 63-HT-34, 1–11.

Davis, E.J., Anderson, G.H., 1966. The incipience of nucleate boiling in forced convection flow. AIChE J. 12, 774–780.

Demiray, F., Kim, J., 2004. Microscale heat transfer measurements during pool boiling of FC-72: effect of subcooling. Int. J. Heat Mass Transfer 47 (14–16), 3257–3268.

Dhir, V.K., 1998. Boiling heat transfer. Annu. Rev. Fluid Mech. 30, 365–401.

Dittus, F.W., Boelter, L.M.K., 1930. Heat Transfer in Automobile Radiators of the Tubular Type, vol. 2. University of California Publication on Engineering. pp. 443–461.

Forster, H.K., Zuber, N., 1955. Dynamics of vapour bubble growth and boiling heat transfer. AIChE J. 1, 531–535.

Henry, C.D., Kim, J., 2004. A study of the effects of heater size, subcooling, and gravity level on pool boiling heat transfer. Int. J. Heat Fluid Flow 25, 262–273.

Incropera, F.P., DeWitt, D.P., 2002. Fundamentals of Heat and Mass Transfer. John Wiley & Sons Inc., New York, USA.

Kandlikar, S.G., 2002. Two-phase flow patterns, pressure drop, and heat transfer during boiling in minichannel flow passages of compact evaporators. Heat Transfer Eng. 23, 5–23.

Kandlikar, S.G., 2004. Heat transfer mechanisms during flow boiling in microchannels. J. Heat Transfer 126, 8–16.

Kim, J.H., You, S.M., Pak, J.Y., 2006. Effects of heater size and working fluids on nucleate boiling heat transfer. Int. J. Heat Mass Transfer 49, 122–131.

Kolev, N.I., 2005. Multiphase Flow Dynamics 2 Thermal and Mechanical Interactions. Springer-Verlag, Berlin, Germany.

Lee, Y., Pioro, I.L., Park, H.J., 1994. An experimental study on a plate type two-phase closed thermosyphon. In: Proc. 4th Int. Heat Pipe Symposium, Tsukuba, Japan.

Mingming, W., Morteza, G., 2002. Experimental studies on the shape and path of small air bubbles rising in clean water. Phys. Fluids 14 (7), L49–L52.

Moghaddam, S., Kiger, K.T., 2004. Pool boiling mechanism of HFE-7100. In: Proc. HT-FED2004, Charlotte, USA.

Mudde, R.F., 2005. Gravity-driven bubbly flows. Annu. Rev. Fluid Mech. 37, 393–423.

Myers, J.G., Yerramilli, V.K., Hussey, S.W., Yee, G.F., Kim, J., 2005. Time and space resolved wall temperature and heat flux measurements during nucleate boiling with constant heat flux boundary conditions. Int. J. Heat Mass Transfer 48 (12), 2429–2442.

Qi, Y., Klausner, J.F., 2006. Comparison of nucleation site density for pool boiling and gas nucleation. J. Heat Transfer 128, 13–20.

Raykoff, T., Kandlikar, S.G., 1997. Bubble characteristics and convective effects in the flow boiling heat transfer of binary mixtures. In: Eng. Foundation Conf. on Convective and Pool Boiling, Irsee, Germany.

Rohsenow, W.M., 1971. Boiling. Annu. Rev. Fluid Mech. 3 (1971), 211–236.

Sakashita, H., Kumada, T., 2001. Method for predicting boiling curves of saturated nucleate boiling. Int. J. Heat Mass Transfer 44 (3), 673–682.

Schlünder, E.-U. et al., 1994. VDI-Wärmeatlas. VDI-verlag GmbH, Düsseldorf, Germany.

Steiner, H., Kobor, A., Gebhard, L.A., 2005. Wall heat transfer model for subcooled boiling flow. Int. J. Heat Mass Transfer 48, 4161–4173.

Vinayak Rao, G., Balakrishnan, A.R., 2004. Heat transfer in nucleate pool boiling of multicomponent mixtures. Exp. Therm. Fluid Sci. 29, 87–103.

Wu, W.-T., Yang, Y.-M., Maa, J.-R., 1998. Nucleate pool boiling enhancement by means of surfactant additives. Exp. Therm. Fluid Sci. 18, 195–209.

Zhang, L., Shoji, M., 2003. Nucleation site interaction in pool boiling on the artificial surface. Int. J. Heat Mass Transfer 46, 513–522.

Zhao, Y., Tsuruta, T., Ji, C., 2003. Experimental study of nucleate boiling heat transfer enhancement in confined space. Exp. Therm. Fluid Sci. 28, 9–16.